

# On the additivity of climate response to anthropogenic aerosols and CO<sub>2</sub>, and the enhancement of future global warming by carbonaceous aerosols

By ALF KIRKEVÅG<sup>1,2\*</sup>, TROND IVERSEN<sup>1,2</sup>, JÓN EGILL KRISTJÁNSSON<sup>1</sup>, ØYVIND SELAND<sup>1,2</sup> and JENS BOLDINGH DEBERNARD<sup>2</sup>, <sup>1</sup>Department of Geosciences, University of Oslo, P.O. Box 1022, Blindern, 0315 Oslo, Norway; <sup>2</sup>Norwegian Meteorological Institute, P.O. Box 43, Blindern, 0313 Oslo, Norway

(Manuscript received 17 April 2007; in final form 10 December 2007)

## ABSTRACT

Climate responses to aerosol forcing at present-day and doubled CO<sub>2</sub>-levels are studied based on equilibrium simulations with the CCM-Oslo atmospheric GCM coupled to a slab ocean. Aerosols interact on-line with meteorology through life-cycling of sulphate and black carbon (BC), and tables for aerosol optics and CCN activation. Anthropogenic aerosols counteract the warming by CO<sub>2</sub> through a negative radiative forcing dominated by the indirect effect. Anthropogenic aerosols reduce precipitation by 4%, while CO<sub>2</sub> doubling gives a 5% increase, mainly through enhanced convective activity, including a narrower ITCZ. Globally, the aerosol cooling is insensitive to CO<sub>2</sub>, and the effects of CO<sub>2</sub> doubling are insensitive to aerosols. Hence, global climate responses to these sources of forcing are almost additive, although sulphate and BC burdens are slightly increased due to reduced stratiform precipitation over major anthropogenic source regions and a modified ITCZ. Regionally, positive cloud feedbacks give up to 5 K stronger aerosol cooling at present-day CO<sub>2</sub> than after CO<sub>2</sub> doubling. Aerosol emissions projected for year-2100 (SRES A2) strongly increase BC and change the sign of the direct effect. This results in a 0.3 K warming and 0.1% increase in precipitation compared to the year 2000, thus enhancing the global warming by greenhouse gases.

## 1. Introduction

There is now little doubt that the increased concentrations of man-made greenhouse gases have caused and will continue to cause a significant global warming (Teng et al., 2006). Important uncertainty still exists concerning the size of the climate response to external forcing, and inaccuracies associated with aerosols and clouds are important in this regard (Andreae et al., 2005; Randall et al., 2007). Aerosols affect climate *directly* by reflecting and absorbing radiation, mainly in the shortwave. The *indirect effects* of aerosols are caused by their altering the number and size of cloud droplets when activated as cloud condensation nuclei (CCN), or by changing the properties of cold clouds, for example, when serving as ice nuclei.

In this paper, we study the equilibrium climate response to the forcing imposed on the climate system by CO<sub>2</sub>-doubling, and by the joint changes in direct and indirect aerosol effects since pre-industrial times. The responses to the greenhouse and the

aerosol forcings are studied both separately and combined. Our experimental tool is an atmospheric General Circulation Model (GCM) coupled to a slab ocean model. The obtained stationary statistics for climate variability during global long-term radiative equilibrium on top of the atmosphere, is assumed to represent the real climate for the given atmospheric composition. Aerosols are included in the GCM with on-line feedbacks. Similar model configurations have been used in several previous papers for studying the climate response to aerosol forcing or combined aerosol and greenhouse forcing using new and sophisticated methods (e.g. Williams et al., 2001; Rotstayn and Lohmann, 2002; Feichter et al., 2004; Kristjánsson et al., 2005; Takemura et al., 2005). Furthermore, it is presently standard procedure to use an atmospheric GCM coupled to a slab ocean for determining equilibrium climate sensitivity and response (e.g. Hegerl et al., 2007). The aim is to investigate the effects in a fully coupled climate model, but important properties can be studied preliminarily with the present type of configuration of experiments. While only fully coupled climate models with a dynamical ocean can yield realistic predictions of future climate development over time, their excessive computational cost render their applicability low in the research phase of new developments.

---

\*Corresponding author.  
e-mail: alf.kirkevag@met.no  
DOI: 10.1111/j.1600-0870.2008.00308.x

A focus of this study is to investigate to what extent climate responds differently to anthropogenic aerosol forcing under different atmospheric CO<sub>2</sub> levels, and conversely, how the equilibrium climate response to CO<sub>2</sub>-doubling varies with aerosol-climate effects. The potential additivity of climate response signals from the two types of forcing is one aspect of this. The issue is tied to the considerable uncertainty of the cloud-radiation feedback in the presence of greenhouse gas forcing, raised by, for example, Stocker et al. (2001, p. 430) and reconfirmed in Randall et al. (2007).

The first studies investigating the equilibrium climate response to the forcing of anthropogenic aerosols included on-line in the GCMs, dealt exclusively with the indirect aerosol effects (Rotstayn et al., 2000; Williams et al., 2001; Rotstayn and Lohmann, 2002). Qualitatively, they agreed on a substantial cooling at mid- and high-latitudes in the Northern Hemisphere and a southward shift of the Intertropical Convergence Zone (ITCZ). The shift in the ITCZ was caused by a stronger cooling in the Northern Hemisphere (NH) than in the Southern Hemisphere (SH), while the cooling at high latitudes was due to positive feedbacks with snow-cover and sea-ice (Williams et al., 2001). Broccoli et al. (2006) found similar responses of the ITCZ on widely different time scales, caused by a range of mechanisms producing interhemispheric temperature contrasts. They concluded that changes in atmospheric heat exchange between the tropics and mid-latitudes are the likely cause of this response. In Feichter et al. (2004), Takemura et al. (2005) and Kristjánsson et al. (2005), the combined response to direct and indirect aerosol forcing was estimated. All the above studies found a southward shift of the ITCZ but least pronounced by Feichter et al. (2004), who used a complex treatment of cloud droplet nucleation with reduced importance of sulphate aerosols compared to simpler schemes (cf. Lohmann and Feichter 2005; Penner et al., 2006; Storelvmo et al., 2006b). Consistently with Chung and Seinfeld (2005), Kristjánsson et al. (2005) found that the direct effect alone causes a southward shift of the ITCZ, but much weaker than the indirect effect. The response to combined aerosol and greenhouse gas forcings was investigated by Feichter et al. (2004) and Rotstayn et al. (2007). The latter simulated an increase in Australian rainfall over the 20th century, consistently with observations, and showed this to be related to increasing aerosol burden over Asia, changing the large-scale atmospheric circulation patterns. Feichter et al. (2004) highlighted non-linear aspects of the responses to aerosol and greenhouse gas forcings, especially on the hydrological cycle. Below we present results from the same kind of calculation from our model, which turn out to be quite different from theirs.

In the composite study by Schulz et al. (2006), nine different global models gave a direct anthropogenic aerosol forcing at the top of the atmosphere (TOA) of  $-0.22 \pm 0.16 \text{ W m}^{-2}$ , while the corresponding values at the ground surface were  $-1.02 \pm 0.23 \text{ W m}^{-2}$ . In the summary for policymakers to the fourth Assessment Report from the Intergovernmental Panel on Climate Change

(IPCC, 2007), the TOA global radiative forcing due to the direct aerosol effect is reported in the range  $-0.1$  to  $-0.9 \text{ W m}^{-2}$  with a best estimate of  $-0.5 \text{ W m}^{-2}$ . The level of scientific understanding is characterized as low to medium. In the same report, the global indirect aerosol forcing is given between  $-0.3$  and  $-1.8 \text{ W m}^{-2}$ , with a best estimate of about  $-0.7 \text{ W m}^{-2}$ . The level of scientific understanding is evaluated as for the direct effect, and thus slightly higher than in the third assessment report (Ramaswamy, 2001). Still, only the first indirect effect (changes in cloud droplet size and number) is considered. The second (lifetime) indirect effect (changes in cloud liquid water path) is considered to have too low level of scientific understanding to be quantified. In the last few years, the range of indirect forcing estimates has started to narrow. Estimates, which include detailed cloud activation and aerosol treatments, tend to lie in the range of  $-0.3$  to  $-1.4 \text{ W m}^{-2}$  (Lohmann and Feichter, 2005). These rather low estimates appear to be more in line with satellite retrievals than the higher estimates, although the uncertainty is still large (Quaas et al., 2006; Storelvmo et al., 2006a).

An important difference between this work and many similar studies on aerosol-climate interactions, is that we use a process-based treatment of internal vs. external mixing of aerosols, while most other models make simpler assumptions on the mixing state (see, e.g. Textor et al., 2006). The state of mixing is in CCM-Oslo parametrized by physio-chemical processes, and may thus also vary with particle size. The size-resolved aerosol composition and number concentration determine the relative importance of aerosol scattering vs. absorption, as well as hygroscopic properties, which in turn affect the nucleation of cloud droplets. The processes leading to internal mixing are therefore crucially important for the results of the climate simulations.

The next section gives a brief review of the model tool that we use, in particular the treatment of aerosols, and describes the setup for the experiments. The main results of these experiments and their interpretation are presented in Sections 3 and 4. Finally, Section 5 presents a summary and the main conclusions.

## 2. Model and experimental setup

### 2.1. The CCM-Oslo with a slab ocean

We use the same model tool for the experiments as in the Kristjánsson et al. (2005) study referred to above, that is, the CCM-Oslo atmospheric climate model coupled to a slab ocean model. CCM-Oslo is a modified version of the NCAR Community Climate Model version 3 (CCM3; Kiehl et al. 1998), which is run at T42 spectral truncation and 18 levels in the vertical. The modifications to the CCM3 include a prognostic cloud water scheme (Rasch and Kristjánsson, 1998), a detailed scheme for aerosol production, transport and deposition (Iversen and Seland, 2002, 2003), a parametrization of aerosol physics, optics and water uptake (Kirkevåg and Iversen, 2002), and a diagnosis of cloud droplet number and size from the aerosols using

prescribed supersaturations, including the effect of cloud droplet size on the release of precipitation in warm clouds (Kristjánsson, 2002). The calculated forcing produced by aerosols influences the modelled atmospheric dynamics and its interaction with the slab ocean. These influences may further change the aerosol distribution and thus the aerosol forcing itself (e.g. Iversen et al., 2005). The coupling of CCM3 to a slab ocean model was described in detail by Kiehl et al. (1996).

Optical parameters and CDNC are in CCM-Oslo calculated by use of pre-calculated look-up tables. The table entries are calculated with a single air parcel model for a wide range of conditions determining size-distributed particle composition, and physical properties from Mie- and Köhler-theory. Basis for the look-up tables are prescribed background aerosol size distributions for primary particles from marine and continental origins (Kirkevåg and Iversen, 2002). These initial multilog-normal size-distributed background aerosols are modified by internal mixing with natural and anthropogenic sulphate and BC, brought about by condensation and coagulation in clear and cloudy air, as well as by wet-phase chemical processes in cloud droplets. Minor fractions of sulphate and BC are assumed externally mixed when emitted as primary particles or chemically produced and then nucleated in clear-air. At increasing relative humidities below 100%, hygroscopic aerosol particles grow by humidity swelling. While cloud droplet number in many studies (e.g. Menon et al., 2002; Rotstain et al., 2007) is diagnosed from empirical relationships between aerosol mass and cloud droplet number, in CCM-Oslo the cloud droplet number is explicitly calculated from the number and physical properties of hygroscopic aerosols, as follows: Cloud condensation nuclei (CCN) are activated by assuming certain maximum supersaturations. We use 0.05% in stratiform clouds, 0.10% in convective clouds over ocean, and 0.15% in convective clouds over land. The cloud droplet number is assumed to equal the concentration of activated CCN. For a more detailed description of the scheme for cloud droplet number concentrations, see Kristjánsson (2002) or Kristjánsson et al. (2005).

A weakness of the present aerosol scheme is the missing explicit treatment of organic carbon (OC) particles, a potentially important component of the global aerosol (e.g. Kanakidou et al., 2005). In more recent versions of the aerosol scheme in CCM-Oslo (Kirkevåg et al., 2005) and CAM-Oslo (Storelvmo et al., 2006b; Seland et al., 2008, *this issue*), OC has been incorporated. Moreover, CAM-Oslo does not use a prescribed background aerosol, but a full scheme for marine and continental natural aerosols. Except in some test simulations for calculations of radiative forcing, diagnostic rather than prognostic supersaturations are used also in that version of CAM-Oslo, however.

## 2.2. Experiments

Combinations of three different aerosol emission scenarios and two chosen levels of CO<sub>2</sub> concentrations define our five experi-

*Table 1.* A schematic overview of the experimental setup. All the experiments are carried out using an interactive slab ocean, as well on-line calculations of aerosol chemistry and transport, with both the direct and indirect effects taken into account

Experiment	Anthropogenic aerosols	Natural aerosols	CO <sub>2</sub> concentrations
NAT1	No	Yes	Present-day
TOT1	2000 emissions	Yes	Present-day
NAT2	No	Yes	2 × present-day
TOT2	2000 emissions	Yes	2 × present-day
FUT2	2100 scenario	Yes	2 × present-day

ments. Aerosol and aerosol precursor emissions for the historical year 2000 (TOT) and the SRES A2 scenario for the future year 2100 (FUT) are as used in Iversen and Seland (2002, 2003) and in IPCC TAR (Penner, 2001). Continuous emissions from volcanism and a 10% fraction of the year 2000 emissions from biomass burning are assumed natural (NAT), whilst the remaining (fossil fuel combustion, biomass burning, and industrial releases) are assumed anthropogenic. The two levels of CO<sub>2</sub> concentrations are (1) the 1990 ('present-day') value from IPCC (2001) at 355 ppmv and (2) the doubled level of 710 ppmv.

The five experiments are thus uniquely denoted by combining the three-letter code for aerosol emissions with the number denoting the CO<sub>2</sub> levels: NAT1, TOT1, NAT2, TOT2 and FUT2. Experiment NAT1 combines natural aerosols with present-day CO<sub>2</sub> levels, while TOT1 uses present-day CO<sub>2</sub> levels and total year 2000 aerosol emissions. [NAT1 and TOT1 are identical to ALLNAT and ALLTOT in Kristjánsson et al. (2005).] The remaining three experiments are all carried out at doubled CO<sub>2</sub> levels; NAT2 is run with natural aerosols, TOT2 with total present-day aerosols, and finally FUT2 with the IPCC SRES A2 aerosol emissions for the year 2100. Note that FUT1 is considered unrealistic and is not included.

For each experiment, the climate reaches approximate radiative equilibrium at the top of the atmosphere (TOA) after a period of about 10 yr, and we use the last 40 yr out of each 50-yr simulation to analyse the equilibrium climate response to a forcing. Table 1 gives a schematic overview of all the simulations, and explains the differences in their setup. We neglect interannual autocovariance and remove signals in temperature and precipitation which, according to the standard *t*-test, are not significant at the 5% level (e.g. von Storch and Zwiers, 1999). Hence, results which are not statistically significant are shown as white patches in Figs. 4, 6, 7, 9 and 10.

## 3. Changes in aerosol burdens and direct radiative forcing

The horizontal distributions of anthropogenic sulphate and black carbon (BC) column burdens for years 11–50 (Fig. 1a) are similar

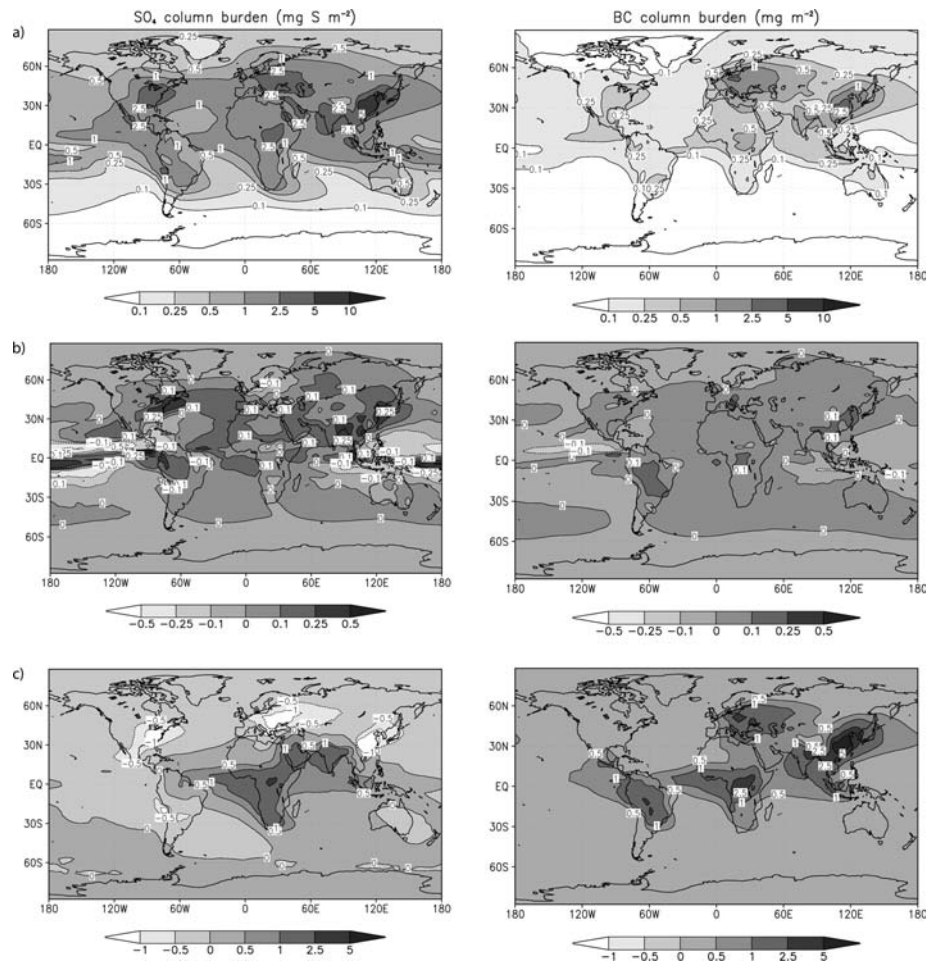


Fig. 1. Simulated change in column integrated mass of sulphate ( $\text{mg S m}^{-2}$ ) (left-hand side) and BC ( $\text{mg m}^{-2}$ ) (right-hand side) due to (Note the difference in scale between a, b and c): (a) Present-day anthropogenic aerosols (exp. TOT1 – NAT1). (b) Doubling of  $\text{CO}_2$  concentrations (exp. TOT2 – TOT1). (c) Year-2100 – present-day aerosols (exp. FUT2 – TOT2).

to those found in the off-line simulations in Iversen and Seland (2002, 2003), except for a southward shift in the tropics, discussed in detail by Kristjánsson et al. (2005). Large sulphate and BC column burdens are calculated over SE Asia, Europe, North America and central Africa. The burdens are much higher in the Northern than in the Southern Hemisphere, see Table 2. The large BC-fraction of emissions from tropical biomass burning relative to NH fossil fuel combustion causes a smaller inter-hemispheric difference for BC than for sulphate. Table 2 also shows that the direct radiative ‘forcing’ (DRF) due to anthropogenic sulphate and BC (the difference TOT1 – NAT1, i.e. a quasi-forcing) is about  $-0.1 \text{ Wm}^{-2}$  in the present response simulations, very close to the DRF in Kirkevåg and Iversen (2002). Due to the considerable computational costs associated with extra calls to the cloud and radiative transfer code, similar (first and second) indirect radiative forcing values have not been explicitly extracted. In Kristjánsson (2002) (the basis for the climate response simulations in Kristjánsson et al., 2005), the indirect

radiative forcing was estimated at  $-1.3 \text{ Wm}^{-2}$  for the first effect, and  $-1.8 \text{ Wm}^{-2}$  for the joint first and second indirect effect. Note that the term forcing is here, as in Kirkevåg and Iversen (2002) and Kristjánsson (2002), used slightly differently than by IPCC-conventions: values are calculated at the top of the atmosphere (TOA) and at the surface. The DRF at a given vertical level is calculated as the increment in net radiative flux due to changes in aerosol optical properties relative to an atmosphere that only contains a prescribed background aerosol consisting of primary particles of natural origins, dominated by sea-salt and mineral dust. The DRF of natural (from DMS, volcanoes, and wildfires) and anthropogenic (from fossil fuel and biomass burning) sulphate and BC are thus calculated separately.

When  $\text{CO}_2$  concentrations are doubled while aerosol and precursor emissions are unchanged (TOT2 – TOT1, Fig. 1b), the simulated sulphate column burdens increase by about 2% in the Northern Hemisphere, but remain unchanged in the Southern. For BC the respective increases are 2 and 3%, see Table 2. These

Table 2. Global and hemispheric averages of key quantities in the experiments defined in Table 1

	Vertically integrated SO <sub>4</sub> column (mg S m <sup>-2</sup> )	Vertically integrated BC column (mg C m <sup>-2</sup> )	DRF (at the TOA) (W m <sup>-2</sup> )	DRFS (DRF at the surface) (W m <sup>-2</sup> )	SWCF (SW cloud forcing) (W m <sup>-2</sup> )	LWCF (LW cloud forcing) (W m <sup>-2</sup> )	SWCF + LWCF (W m <sup>-2</sup> )
<b>NAT1</b>							
<b>global</b>	0.228	0.135	-0.089	-0.119	-47.82	29.07	-18.75
<b>NH</b>	0.243	0.129	-0.095	-0.125	-48.10	30.01	-18.09
<b>SH</b>	0.212	0.141	-0.083	-0.113	-47.55	28.13	-19.42
<b>TOT1</b>							
<b>global</b>	1.196	0.341	-0.198	-0.824	-48.67	28.55	-20.12
<b>NH</b>	1.683	0.468	-0.247	-1.101	-48.65	27.98	-20.67
<b>SH</b>	0.709	0.214	-0.150	-0.546	-48.69	29.13	-19.57
<b>NAT2</b>							
<b>global</b>	0.231	0.142	-0.089	-0.121	-48.66	29.28	-19.38
<b>NH</b>	0.245	0.131	-0.093	-0.124	-48.60	29.99	-18.61
<b>SH</b>	0.217	0.152	-0.085	-0.117	-48.73	28.58	-20.15
<b>TOT2</b>							
<b>global</b>	1.214	0.349	-0.190	-0.824	-49.30	28.83	-20.46
<b>NH</b>	1.719	0.477	-0.235	-1.095	-48.93	28.10	-20.83
<b>SH</b>	0.709	0.221	-0.145	-0.554	-49.66	29.56	-20.10
<b>FUT2</b>							
<b>global</b>	1.277	0.830	0.115	-1.312	-49.23	28.90	-20.33
<b>NH</b>	1.735	1.165	0.246	-1.746	-48.86	28.44	-20.42
<b>SH</b>	0.820	0.494	-0.016	-0.878	-49.61	29.36	-20.25

Note: The short-wave direct radiative forcing data (DRF, due to sulphate and BC) are taken from the last 8 years of the simulations. Furthermore, the short-wave cloud forcing (SWCF) is based on radiative transfer calculations with the aerosol optics taken into account, meaning that a (small) clear-sky direct effect contribution is embedded in the SWCF.

results are parts of climate responses to CO<sub>2</sub>-doubling which involve altered circulation, cloud, precipitation and aerosol feedbacks (cf. Iversen et al., 2005), which are discussed in the next section. The respective change in DRF due to anthropogenic aerosols is only about +0.01 Wm<sup>-2</sup> for both hemispheres.

If CO<sub>2</sub> concentrations are kept constant at doubled level but aerosol emissions change from present-day to year 2100 levels (i.e. FUT2 – TOT2, Fig. 1c), the global column burden of BC is more than doubled, whilst that for sulphate only increases by ca. 5% (Table 2). Compared to the present-day situation, the sulphate burden is shifted southwards in the 2100 scenario. The vertical and meridional variation of the zonally averaged direct forcing is shown in Fig. 2. Aerosol absorption of solar radiation is large where the vertical forcing gradient is large. This occurs in the lowermost 5 km of the troposphere in the tropical and mid-latitude NH both for the anthropogenic contribution to present-day aerosols (Fig. 2a) and for the contribution by aerosol changes from present-day to the 2100 scenario (Fig. 2b). However, the absorption is larger in the latter case due to the large increase in BC concentrations in the 2100 scenario.

Figures 3a and b show the change in DRF from present-day to year-2100 at the TOA and the surface, respectively. Due to the importance of shortwave absorption by BC in regions with

high albedo below, at the TOA (Fig. 3a) there is a substantial increase in DRF, with a global average of +0.31 W m<sup>-2</sup> (Table 2). This is even 0.2 W m<sup>-2</sup> larger than the estimated DRF itself in Kirkevåg and Iversen (2002). Regionally, contributions are of both signs due to the southward shift of sulphate (Fig. 1c). The largest increase, exceeding 5 W m<sup>-2</sup>, is found over SE Asia, but the increase is also considerable in eastern Europe and in areas dominated by biomass burning in S-America and Africa, with values between 1 and 2 W m<sup>-2</sup>. The values in the Southern Hemisphere are generally smaller due to fewer and weaker emission sources, and in southern Africa the changes are negative, due to enhanced contributions from sulphate there (Fig. 1c).

Contrary to the TOA, the ground surface DRF (Fig. 3b) shows a substantial negative change over the four geographical regions just mentioned, peaking at about -4 W m<sup>-2</sup> in central Africa and parts of SE Asia. The globally averaged change is -0.49 W m<sup>-2</sup> (Table 2). Polewards of 60°N and 40°S the changes are considerably smaller, due to smaller aerosol burdens and weaker solar insolation there. (Note that at high NH latitudes, both sulphate and BC are probably underestimated by the model, see Iversen and Seland, 2002, 2003). Since the hydrological cycle is basically driven by an energy surplus at the ground surface relative

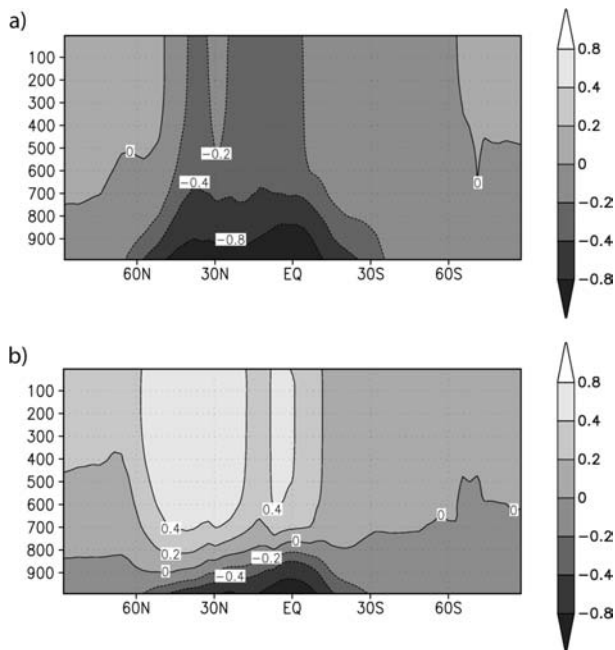


Fig. 2. Vertical cross-section of the zonally averaged direct radiative forcing ( $\text{W m}^{-2}$ ) by anthropogenic aerosols in the following cases: (a) Present-day total – natural aerosols at double  $\text{CO}_2$  (exp. TOT2 – NAT2). (b) Year-2100 – present-day total aerosols at double  $\text{CO}_2$  (exp. FUT2 – TOT2).

to the atmosphere, due to radiative processes, the negative DRF change seen in Fig. 3b may be expected to influence evaporation and precipitation. We will discuss this issue in the next section.

For changes in indirect forcing between the years 2000 and 2100, we refer to Kristjánsson (2002). As shown in Fig. 10b of that paper, the globally averaged indirect forcing is virtually unchanged, while there are significant regional changes such as, for example, a negative forcing change over Africa and a positive forcing change over eastern Europe. The large increase of BC during the 21st century was found to have a minor influence on the aerosol indirect forcing.

## 4. Changes in atmospheric climate

### 4.1. The response to aerosol forcing

Globally averaged we estimate negligible interactions between aerosol effects and the effects of doubling  $\text{CO}_2$ . We find a global surface air cooling of 1.44 K and a 4.2% decrease in global precipitation due to anthropogenic aerosols at present-day  $\text{CO}_2$  levels (TOT1 – NAT1). The corresponding figures at doubled  $\text{CO}_2$  (TOT2 – NAT2) are 1.46 K and 4.0%, respectively. At both present-day and doubled  $\text{CO}_2$  levels the largest temperature reductions are found in the Northern Hemisphere, as a consequence of the larger aerosol burdens compared to the Southern Hemisphere. Consequently, the southward displacement of the

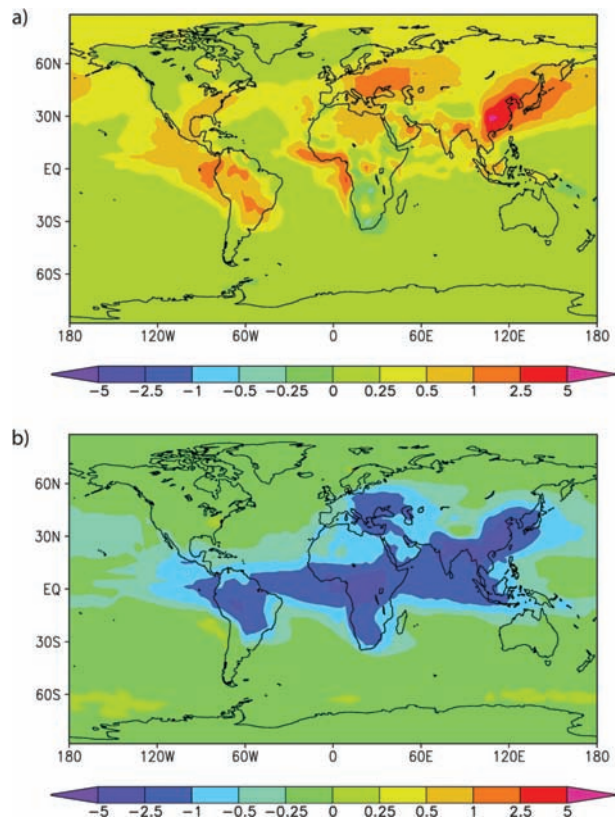


Fig. 3. Change in direct radiative forcing (in  $\text{W m}^{-2}$ ) during the 21st century due to changes in aerosol optical properties (FUT2 – TOT2): (a) At TOA. (b) At the surface.

Intertropical Convergence Zone (ITCZ) found in Kristjánsson et al. (2005) is reproduced here (Figs. 4a and b), implying considerable regional changes such as drying of the Sahel region in Africa. This result is also consistent with a range of studies referred to in the introduction. The general reduction in precipitation (see Table 3) is a combined consequence of a reduced hydrological cycle in the colder climate, and the slower auto-conversion of cloud water to rain in warm clouds when droplets become smaller (the second indirect effect, cf. Kristjánsson, 2002).

Since the sulphate burden is only slightly increased and BC is more than doubled in the year 2100 aerosol emission scenario, we estimate a global 0.32 K warming and a 0.1% increase in precipitation compared to present-day values (i.e. FUT2 – TOT2, see Table 3). The equilibrium temperature response in Fig. 4c is consistent with the increased TOA forcing (Fig. 3a), but the unchanged globally averaged precipitation (Table 3) reflects the reduced forcing at the surface (Fig. 3b). Furthermore, the cooling by anthropogenic aerosols in 2100 is reduced more in the Northern Hemisphere (0.44 K) than in the Southern (0.20 K), and the southward shift in ITCZ is therefore somewhat reversed (Fig. 4c).

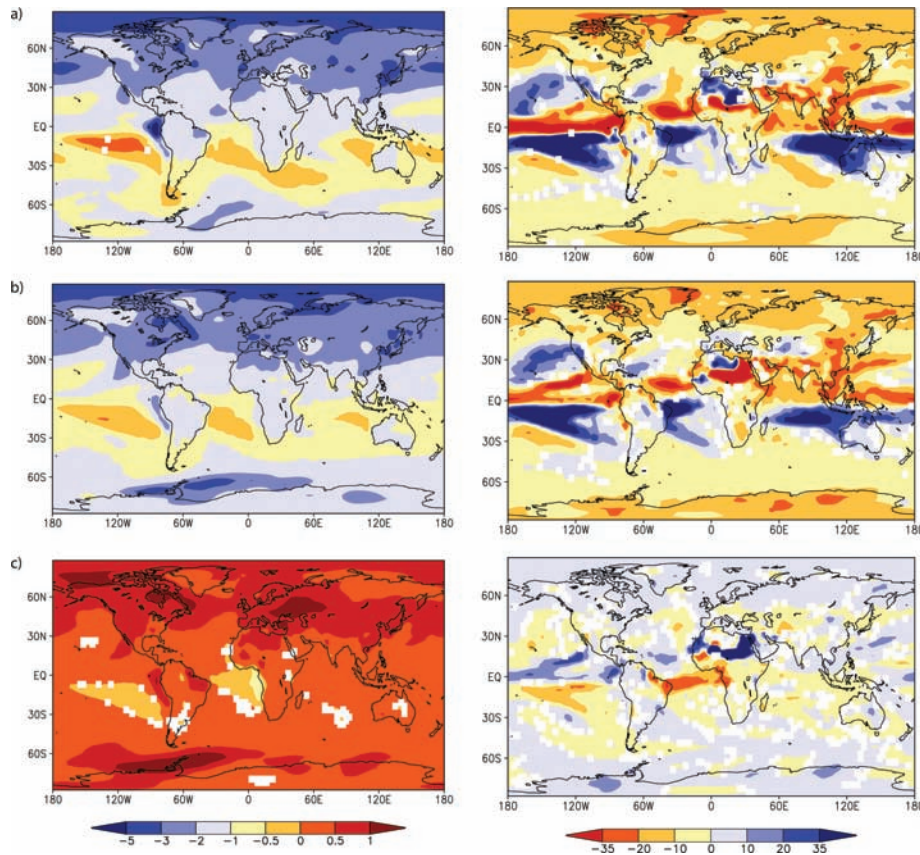


Fig. 4. Estimated influence of aerosols on the surface air temperatures (K, left-hand side) and precipitation (% , right-hand side): (a) Present-day total – natural aerosols at present-day CO<sub>2</sub> (exp. TOT1 – NAT1). (b) Present-day total – natural aerosols at doubled CO<sub>2</sub> (exp. TOT2 – NAT2). (c) Year-2100 – present-day aerosols at doubled CO<sub>2</sub> (exp. FUT2 – TOT2).

In agreement with results from similar climate simulations (Williams et al., 2001; Rotstajn and Lohmann, 2002), the response pattern for temperature differs considerably from the forcing pattern. A considerable part of the response is a consequence of local feedback processes driven by horizontal fluxes of energy rather than the forcing directly (Boer and Yu, 2003). Whilst the negative forcing by anthropogenic aerosols is pronounced at low and mid-latitudes of the Northern Hemisphere (Kirkevåg and Iversen 2002; Kristjánsson 2002), the response exhibits cooling peaking at high latitudes (Figs. 4a and b and 5a). The response reflects in particular feedbacks connected with the influence of sea-ice and snow-cover on the ground surface albedo and heat fluxes. A negative cloud feedback tends to dampen the Arctic signal (Kristjánsson et al., 2005). There is also a signature of larger cooling over NH continents than oceans (Figs. 4a and b), reflecting the difference in ground surface heat capacity and the cold-ocean warm-land atmospheric flow pattern with a negative sign (Wallace et al., 1996). This is in agreement with the view that small forcing perturbations do not alter the structure of dynamical flow regimes in the climate system, but only influence their relative frequency of occurrence (Corti et al., 1999; Palmer, 1999; Iversen et al., 2008). Although with opposite sign, these

response patterns are similar to those of CO<sub>2</sub>-doubling (Figs. 5b and 6), and to the differences between the 2100 aerosol scenario and that of the present-day (FUT2 – TOT2), see Fig. 4c.

#### 4.2. Response to doubling of CO<sub>2</sub>

When CO<sub>2</sub> concentrations are doubled while aerosol emissions are kept constant, the global equilibrium response is a 2.61 K warming and a 4.5% precipitation increase for natural aerosols, and 2.58 K and 4.8%, respectively, for total aerosols in the year 2000. Hence, for the global net response, non-linear interactions between CO<sub>2</sub> driven and aerosol driven effects are largely negligible. These responses indicate that CCM-Oslo has a higher equilibrium climate sensitivity (ECS) than NCAR CCM3. For the standard version of CCM3 coupled to a slab ocean, Meehl et al. (2000) estimated 2.08 K and 3.9% for surface air temperature and precipitation, respectively. In a version of CCM3 using the same prognostic cloud water scheme as in the present study, but without the link to the radiation and aerosol schemes that we have introduced (Kristjánsson, 2002), the temperature response was only 1.96 K. Assuming an approximate radiative forcing of 3.5 W m<sup>-2</sup> due to doubling of CO<sub>2</sub>, as in Meehl et al. (2000), the

*Table 3.* Global and hemispheric averages of key quantities in the experiments defined in Table 1. Surface air temperature is defined as the temperature at reference height in the model (2 m above the ground over land). To facilitate comparisons with Kristjánsson et al. (2005) and Kristjánsson (2002), also (radiative) surface temperatures and estimates of effective cloud droplet radii as would be seen from satellite are included.

	Surface temperature (°C)	Surface air temperature (°C)	Precipitation (mm d <sup>-1</sup> )	Cloud cover (%)	Cloud liquid water path (g m <sup>-2</sup> )	Cloud ice water path (g m <sup>-2</sup> )	Effective cloud droplet radius (μm)
<b>NAT1</b>							
global	14.02	12.69	2.89	57.2	41.64	17.17	10.80
NH	14.65	13.36	2.95	58.3	43.19	17.01	10.45
SH	13.40	12.02	2.84	56.0	40.10	17.32	11.14
<b>TOT1</b>							
global	12.60	11.25	2.77	57.2	41.49	17.23	10.13
NH	12.69	11.40	2.58	57.6	43.70	16.63	9.57
SH	12.51	11.11	2.95	56.7	39.28	17.83	10.65
<b>NAT2</b>							
global	16.60	15.30	3.02	57.3	45.58	16.68	10.95
NH	17.18	15.93	3.06	58.4	47.57	16.65	10.57
SH	16.02	14.68	2.99	56.2	43.60	16.71	11.31
<b>TOT2</b>							
global	15.14	13.84	2.90	57.2	45.51	17.01	10.26
NH	15.29	14.04	2.69	57.5	48.38	16.54	9.67
SH	15.00	13.64	3.11	56.9	42.65	17.47	10.83
<b>FUT2</b>							
global	15.46	14.16	2.90	57.2	45.55	16.85	10.29
NH	15.73	14.48	2.73	57.7	48.15	16.43	9.72
SH	15.19	13.84	3.07	56.7	42.96	17.28	10.83

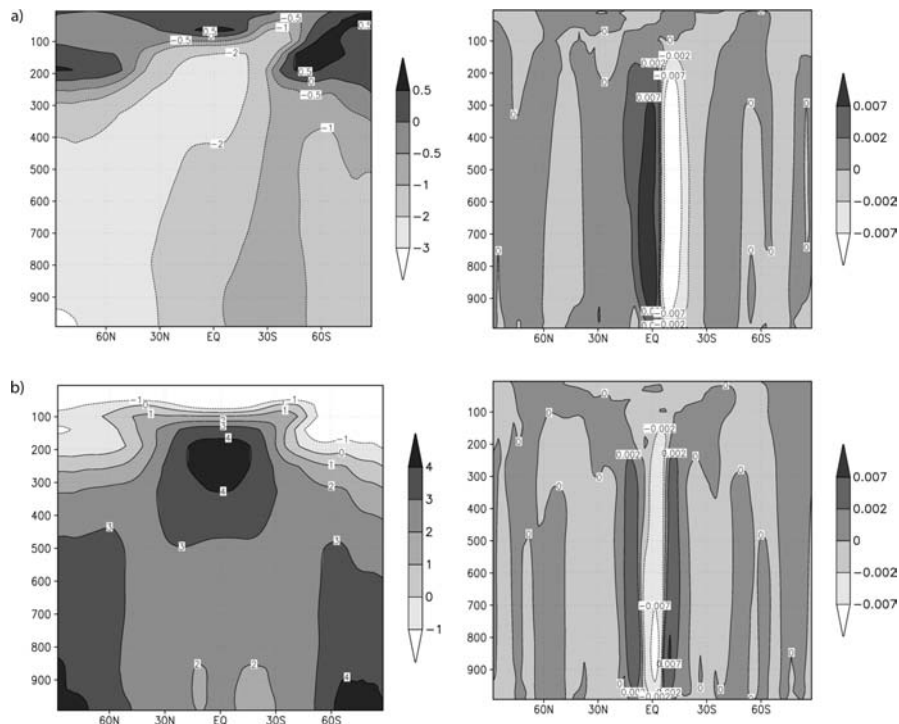


*Fig. 5.* Zonally averaged response in temperature (K, left-hand side) and vertical velocity  $\omega$  (hPa s<sup>-1</sup>, right-hand side) to: (a) The joint aerosol direct and indirect effects at present-day CO<sub>2</sub> levels (exp. TOT1 – NAT1). (b) A doubling of CO<sub>2</sub> at present-day aerosol levels (exp. TOT2 – TOT1).

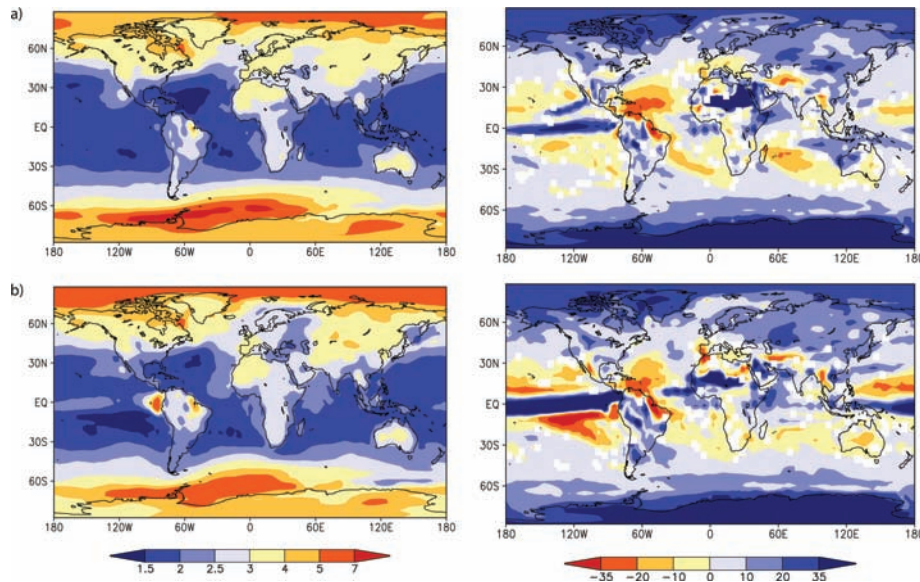


Fig. 6. Estimated influence of a doubling of the CO<sub>2</sub> concentrations on the simulated surface air temperatures (K) (left-hand side) and precipitation (%) (right-hand side): (a) Natural aerosols (exp. NAT2 – NAT1). (b) Present-day total aerosols (exp. TOT2 – TOT1).

ECS for CCM-Oslo becomes 0.74 K/(Wm<sup>-2</sup>), compared to 0.59 and 0.56 K/(Wm<sup>-2</sup>) for the CCM3 versions with diagnostic and prognostic cloud water, respectively.

By comparison, applying the aerosol indirect forcing of  $-1.83 \text{ W m}^{-2}$  found by Kristjánsson (2002) and the direct forcing of  $-0.19 \text{ W m}^{-2}$  from Kirkevåg and Iversen (2002), the calculated cooling by present-day anthropogenic aerosols at present-day CO<sub>2</sub> levels (TOT1 – NAT1) corresponds to an ECS of 0.71 K/(Wm<sup>-2</sup>), that is, close to that for CO<sub>2</sub> forcing. For the direct or the indirect effect separately, the numbers are 0.73 and 0.68 K/(Wm<sup>-2</sup>), respectively (Kristjánsson et al. 2005). Feichter et al. (2004) used the ECHAM4 atmospheric GCM coupled to a slab ocean model in a similar study to ours. They found a substantial 17% K<sup>-1</sup> decrease in the sulphate and BC burdens after an increase in CO<sub>2</sub> from pre-industrial to present-day levels. These reductions were attributed to a shortened aerosol residence time due to increased precipitation in a warmer climate. Contrary to their results, we find slightly increased aerosol burdens when CO<sub>2</sub> levels are doubled, see Fig. 1b. With natural aerosol emissions (NAT2 – NAT1) the increases in sulphate and BC burdens are 0.5 and 2.0% K<sup>-1</sup>, respectively, whilst for present-day aerosol emissions (TOT2 – TOT1) they are 0.6 and 0.9% K<sup>-1</sup> (Tables 2 and 3). Away from regions influenced by the modification of the ITCZ (see Figs. 5b and 6), the increase in aerosol column burden is largest in and downstream of the source regions, see Fig. 1b. In agreement with Feichter et al. (2004), the column burdens are reduced slightly in the most remote regions.

One reason for the difference in BC and sulphate response between our study and that of Feichter et al. (2004) is the different treatment of precipitation scavenging. Their model used a

below-cloud collection efficiency for particles of 0.3 whilst ours is only 0.1 for sulphate produced in aqueous phase and 0.2 for the remaining sulphate and for BC. Underlying these numbers is the assumption that the relatively large accumulation-mode sulphate particles produced in cloud droplets are close to the scavenging gap (Seinfeld and Pandis, 1998, p. 1020). The aqueous phase sulphate was in Iversen and Seland (2002) estimated to constitute the major portion of the total sulphate burden. The cloud water path increases in both studies due to the greenhouse gas forcing, by 3.1% K<sup>-1</sup> in Feichter et al. (2004) and in our study by 2.2% K<sup>-1</sup> for natural aerosols and 2.5% K<sup>-1</sup> for present-day aerosols.

Another important process which influences the response in aerosol burdens is the in-cloud scavenging of contaminants by convective precipitation. In CCM-Oslo, this is effective only in the local convective cloud fraction of any grid volume (Iversen and Seland, 2002). (In CAM-Oslo this has been changed, see Seland et al. 2008). Since convective precipitation intensity frequently is very high, soluble contaminants inside the convective cloud fractions are efficiently removed, and increased precipitation in these fractions hardly increases the scavenged contaminant mass. Consequently, soluble contaminant species are relatively more susceptible to changes in the stratiform precipitation, which is less intense and more widespread. While the global total precipitation increases, the stratiform precipitation changes very little with a doubling of CO<sub>2</sub>. In fact, it is reduced in most of the important source regions for aerosols between 25 and 50°N (Fig. 7). Together with regional reductions in the total precipitation over oceans in the subtropics (see Fig. 6), this leads to a slight increase in life-time and burden of anthropogenic aerosols.

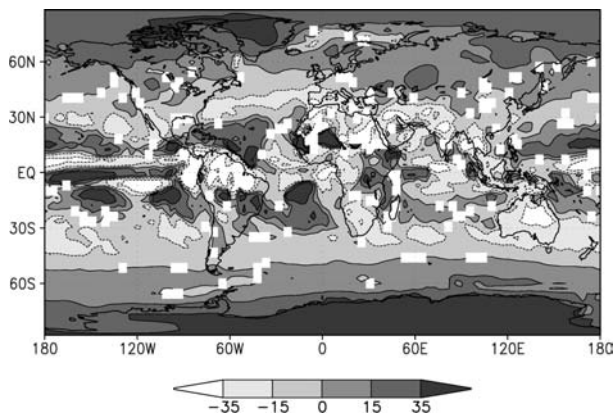


Fig. 7. Increase in stratiform precipitation (%) due to CO<sub>2</sub> doubling (exp. TOT2 – TOT1).

Close to the ITCZ the CO<sub>2</sub> doubling results in changes in precipitation and contaminant burdens (sulphate and BC) which need some explanation. Figure 5b shows that the Hadley circulation is modified. It is well documented that NCAR's CCM3 (Hack et al., 1998), and many other climate models, produce an artificial 'double' ITCZ, in particular over the eastern Pacific (e.g. Zhang, 2001; Zhang and Wang, 2006). In CCM-Oslo the split is increased as a consequence of the southward ITCZ displacement forced by anthropogenic aerosols (Fig. 8a). After CO<sub>2</sub> doubling the centre portion of ITCZ exhibits strengthened rising air motion whilst the increased subtropical subsidence on the flanks results in a narrowing of the ITCZ by a few degrees of latitude and with a reduced split (see Figs. 5b, 7 and 8a). The ITCZ precipitation amount is increased (Fig. 6), but in a considerably narrower zone. The vertical velocity changes in Fig. 5b are associated with increased convergence into the centre portions of ITCZ but increased divergence from the subtropical flanks. Therefore, in spite of the ITCZ precipitation increase, both burdens and deposition of sulphate and BC increase close to the ITCZ and decrease on the flanks (Figs. 1b and 8b).

#### 4.3. Combined response to CO<sub>2</sub> doubling and aerosols

A noteworthy difference between our results and those of Feichter et al. (2004) is the different response of the hydrological cycle to changes in aerosols and CO<sub>2</sub>. The equilibrium hydrological sensitivity (EHS) is defined as  $\Delta P/\Delta T$ , where  $\Delta P$  is the global change in precipitation (%) and  $\Delta T$  the global change in surface air temperature (K) when equilibrium is reached as a response to an external forcing. Feichter et al. (2004) obtained a nearly three times larger EHS for aerosols (3.9% K<sup>-1</sup>) than for CO<sub>2</sub> (1.5% K<sup>-1</sup>), and therefore a *negative* EHS of about -2% K<sup>-1</sup> for the combined changes in aerosols and CO<sub>2</sub> from pre-industrial to present-day levels. Although trends from precipitation observations are only reliable over continents, observations during the 20th century indicate a positive EHS (IPCC,

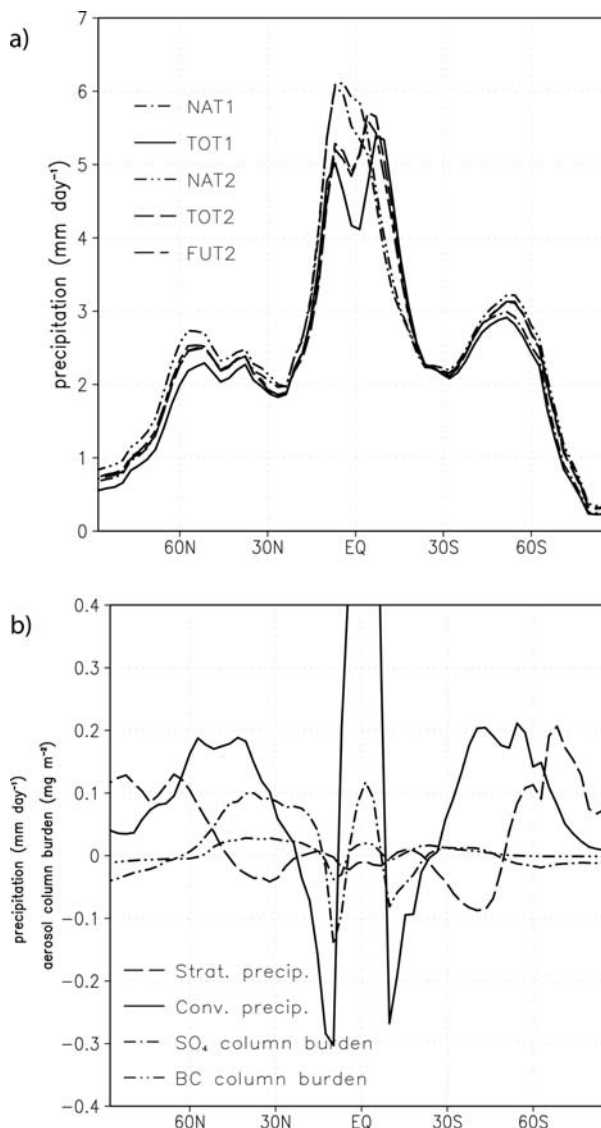


Fig. 8. Zonally averaged precipitation and aerosol burdens. (a) Total precipitation (mm day<sup>-1</sup>) in experiment NAT1, TOT1, NAT2, TOT2 and FUT2. (b) Increase due to CO<sub>2</sub> doubling (exp. TOT2 – TOT1) in stratiform and convective precipitation (with a maximum of 1.1 mm d<sup>-1</sup> at the equator) and column burdens of sulphate (mg S m<sup>-2</sup>) and BC (mg m<sup>-2</sup>).

2001). We calculate a smaller EHS for aerosols and a larger for CO<sub>2</sub> than Feichter et al. (2004). It is estimated to ca. 3.0% K<sup>-1</sup> for present-day anthropogenic aerosols, and 1.8% K<sup>-1</sup> for CO<sub>2</sub> doubling, which is close to the value 1.9% K<sup>-1</sup> given in IPCC (2001). For the joint changes in aerosols and CO<sub>2</sub> we estimate an EHS of 0.30% K<sup>-1</sup> in TOT2 – NAT1, and 0.24% K<sup>-1</sup> in FUT2 – NAT1. This difference in EHS estimated with the same model, suggests that the concept of equilibrium response per TOA forcing can be misleading (e.g. Shine et al., 2003). For FUT2 – TOT1 both anthropogenic aerosols and CO<sub>2</sub> contribute

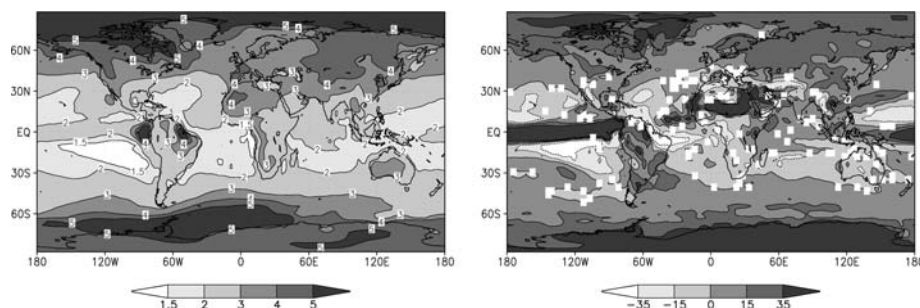


Fig. 9. Estimated influence of combined doubling of the CO<sub>2</sub> concentrations and aerosols on the simulated surface air temperatures (K, left-hand side) and precipitation (% change, right-hand side) for year-2100 – present-day CO<sub>2</sub> and aerosol levels (exp. FUT2 – TOT1).

to a global warming and the EHS is  $1.6\% \text{ K}^{-1}$ , which is close to that of CO<sub>2</sub> alone, see Table 3.

Feichter et al. (2004) also found a considerably smaller global warming for combined anthropogenic aerosol and CO<sub>2</sub> forcing (0.57 K) than obtained by adding the two individual responses (0.85 K). Unlike their results, corresponding to a non-linearity factor of about 49%, we find quasi-linearity in the globally averaged climate response to changes in aerosols and CO<sub>2</sub> in CCM-Oslo: a warming of 1.15 K for the combined forcing and 1.17 K when treating the response to the two forcings separately (see Table 3), corresponding to a global non-linearity factor of less than 2%. For global precipitation, and even for cloud liquid water path, the factor is similar.

Combined effects of future (year 2100) versus year-2000 changes in anthropogenic aerosol and CO<sub>2</sub> (FUT2 – TOT1) on surface air temperature and precipitation are shown in Fig. 9. The average surface air temperature increases by 3.08 K in the Northern Hemisphere, and 2.73 K in the Southern. A particularly large warming is found off the coast of equatorial South America. As discussed further in the next subsection, this is due to a strong reduction in low cloud amount in this region. The precipitation increases by 5.8% and 4.1% in the Northern and Southern Hemispheres, respectively, with values exceeding 20% in parts of northern Europe. In southern Europe, on the other hand, the scenario gives large and significant reductions in precipitation, which is also found for a doubling of CO<sub>2</sub> in Fig. 6. This tendency is seen in many global climate model simulations in response to greenhouse gas forcing (IPCC, 2001), and is probably due to the increased subtropical subsidence associated with the modified Hadley circulation (Fig. 5b). Due to the increase in shortwave-absorbing BC aerosols from year 2000 to 2100, the cooling by present-day anthropogenic aerosols is in most regions switched to a slight warming (relative to present-day) in this future scenario (see Fig. 4c), thus adding to the response to increased CO<sub>2</sub> levels.

#### 4.4. Regional interactions between aerosols and CO<sub>2</sub>

Regionally, the effect of present-day anthropogenic aerosols may enhance the response to CO<sub>2</sub> doubling. For example, the increase

in precipitation in central parts of South America occurs both in Figs. 4a and b, due to aerosols, and in Fig. 6, due to doubled CO<sub>2</sub>. The opposite, a decrease in precipitation, is found in large parts of Africa south of the Sahel, and in smaller regions of southeast Asia. These regions stand out with large, statistically significant changes in precipitation both in TOT2 – NAT1 and in FUT2 – NAT1 (not shown).

In some regions, however, the response to anthropogenic aerosols is considerably different between present-day and doubled CO<sub>2</sub> levels, i.e. TOT2 – NAT2 differs from TOT1 – NAT1 regionally (Figs. 4a and b). This is seen downstream of mid- and high latitude polluted areas in Europe, Asia and North and South America, and over the eastern equatorial Pacific. Over the former four regions, the cooling due to anthropogenic aerosols is up to about 1 K stronger at doubled CO<sub>2</sub> levels than at present CO<sub>2</sub> levels (Fig. 10a), probably associated with increased sulphate burdens due to the mid-latitude reduced stratiform precipitation, as discussed in Section 4.2.

In the equatorial Pacific close to South America, however, the maximum cooling by anthropogenic aerosols is up to about 5 K larger at present-day CO<sub>2</sub> (TOT1 – NAT1  $\approx -7$  K) than after doubling (TOT2 – NAT2  $\approx -2.5$  K). Note that the response increments (TOT2 – TOT1) – (NAT2 – NAT1) are identical to (TOT2 – NAT2) – (TOT1 – NAT1). Therefore, the maximum temperature response to CO<sub>2</sub> doubling off the Peruvian coast (Fig. 6) is also about 5 K larger with present-day aerosols (almost 7 K) than in the simulations with only natural aerosols (about 2.5 K), see Fig. 10a.

In this particular region the response to anthropogenic aerosols in net downward solar irradiance at the ocean surface exceeds  $-60 \text{ Wm}^{-2}$  at present-day CO<sub>2</sub> levels. At doubled CO<sub>2</sub> the response is reduced to about  $-10 \text{ Wm}^{-2}$ , so that the difference due to anthropogenic aerosols increases by about  $50 \text{ Wm}^{-2}$  from present-day to doubled CO<sub>2</sub> levels. The corresponding increase in the aerosol-driven change in net outgoing long-wave irradiances from the ocean surface is only about half of this. Hence anthropogenic aerosols force a much weaker surface cooling in the region at doubled CO<sub>2</sub> than at present-day CO<sub>2</sub> levels. The simulated changes in shortwave and long-wave cloud forcing imply that a major part of the mentioned radiative perturbations in

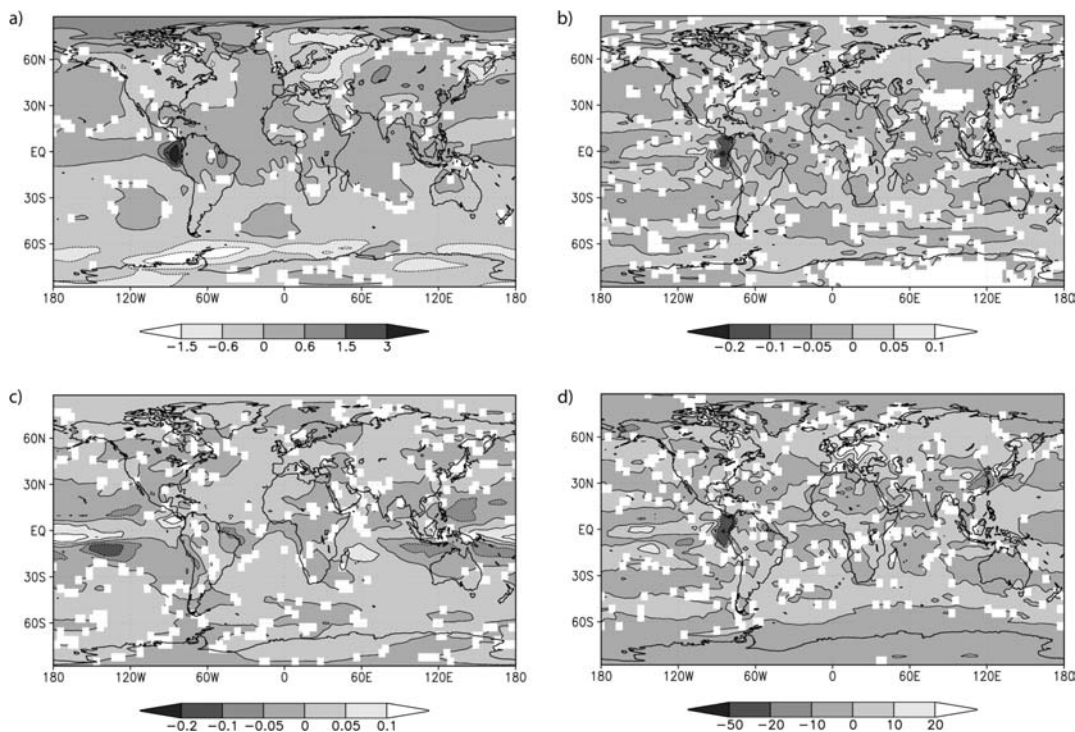


Fig. 10. Difference in the response to a doubling of CO<sub>2</sub> between the simulations with present-day aerosols and the simulations with natural aerosols, that is, TOT2 – TOT1 – (NAT2 – NAT1), or alternatively (an equivalent perspective): difference in the response to anthropogenic aerosols between the simulations with doubled CO<sub>2</sub> and simulations with present-day CO<sub>2</sub>, that is, TOT2 – NAT2 – (TOT1 – NAT1): (a) Surface air temperature (K); (b) low level cloud fraction; (c) high level cloud fraction and (d) vertically integrated liquid water path ( $\text{g m}^{-2}$ ).

this area are indeed due to reduced low-level cloudiness at doubled CO<sub>2</sub>. Figure 10b shows a fractional increase in low-level cloudiness which is more than 0.2 smaller in TOT2 – NAT2 than in TOT1 – NAT1. The respective differences between the high cloud fraction responses, see Fig. 10c, are only about 0.02, and for medium high clouds the differences are even smaller.

Compared to surface observations by Warren et al. (1988) and ISCCP D2 data (Rossow and Schiffer, 1999), our control simulation, TOT1, has up to a factor 2 too large low-level cloud fraction in the eastern equatorial Pacific region. The three simulations NAT1, NAT2 and TOT2 are all in better agreement with the data even though they do not represent the present-day climate situation. This is probably due to underestimated temperatures, which in turn is partly caused by the exaggerated indirect effect in CCM-Oslo (Kristjánsson, 2002). Globally averaged, the surface air temperature (Table 3) is about 3 K lower than in the Legates and Willmott (1990) data, and locally in the region more than 10 K too low. At present-day CO<sub>2</sub> levels the aerosol-driven increase in vertically integrated liquid water path (LWP) in the same region is about 50–60  $\text{g m}^{-2}$ . This is much larger than the 5–10  $\text{g m}^{-2}$  in the corresponding simulations with the aerosol indirect effect alone (fig. 8 in Kristjánsson et al., 2005). It is also much larger (see Fig. 10d) than the 7–15  $\text{g m}^{-2}$  in the same region at doubled CO<sub>2</sub> concentrations, when both the direct and indirect effects are included (i.e. TOT2 – NAT2). In

Kristjánsson (2002) the total indirect forcing over the equatorial Pacific Ocean was dominated by the lifetime effect. The large changes in LWP we find here indicate that the same is true in the present-day CO<sub>2</sub> simulations presented here (TOT1 – NAT1). Without the warming by doubling of CO<sub>2</sub>, the strongly cooling aerosol (mainly lifetime) effect causes the air in the lowest model level to be nearly saturated, giving a strong, and probably exaggerated, increase in the low-level cloud cover. Since low clouds by themselves cool the surface below, this constitutes a positive cloud feedback. This response is probably due to a weakness in the model set-up, for example connected with a missing ability to produce an ENSO response with a slab-ocean model.

The situation for the eastern equatorial Pacific region is very similar to what has been found in Kiehl et al. (2006) for a doubling of CO<sub>2</sub> in an intermediate version of CAM3 and in CCSM3, both using the prognostic cloud water scheme from Rasch and Kristjánsson (1998) as in CCM-Oslo, when the horizontal resolution was increased from T42 to T85. For CAM3 coupled to a slab ocean model this was attributed to over-prediction of cloud fractions in the lowest model level in the control simulation. In this case the persistent near-saturation conditions were due to inefficient mixing of drier air from above. At doubled CO<sub>2</sub> they found a substantial decrease in the low level cloud fraction, leading to an anomalous change in the shortwave cloud forcing. In the CAM3 T42 version used in the fully coupled CCSM3 climate

model, this was controlled by bounding the depth of the boundary layer, but that adjustment did not prevent this behaviour from occurring at the T85 horizontal resolution.

## 5. Summary and conclusions

The equilibrium climate response to the joint aerosol direct and indirect forcing at present-day and doubled CO<sub>2</sub> levels, as well as interactions between the effects of aerosols and CO<sub>2</sub>, have been investigated based on five multidecadal simulations with CCM-Oslo coupled to a slab ocean model. One objective of this study has been to investigate the potential additivity of climate response to forcing by anthropogenic aerosols and increased CO<sub>2</sub>-levels. Another important issue addressed is the role of anthropogenic aerosols in a future scenario for global greenhouse warming.

When CO<sub>2</sub> concentrations are doubled and aerosol emissions are kept constant at natural levels, we estimate a global warming of 2.61 K and an increase in precipitation of 4.5%, compared to 2.58 K and 4.8% with present-day aerosol emissions. Even though non-linear interactions between the effects of CO<sub>2</sub> doubling and anthropogenic aerosols are negligible globally, there are positive cloud feedbacks for low level clouds regionally, especially over the eastern equatorial Pacific Ocean, where surface air temperatures are too cold in the simulation with present-day aerosol emissions and CO<sub>2</sub> concentrations. When CO<sub>2</sub> is doubled, CCM-Oslo yields a small increase in sulphate and BC burdens, globally averaged, despite the almost 5% increase in precipitation. Most of that increase is in the form of convective precipitation, to which wet scavenging of aerosols is relatively insensitive in the model. The simulated stratiform precipitation is almost unchanged in a global mean, but actually decreases in large areas of major aerosol emissions. Together with regionally reduced precipitation over oceans in the subtropics, this leads to a slight increase in the lifetime and burden of anthropogenic aerosols.

However, the global response to anthropogenic aerosol forcing is found to be nearly independent of the CO<sub>2</sub> level. For present-day CO<sub>2</sub> the surface air cooling is estimated at 1.44 K, accompanied by a 4.2% decrease in precipitation, while the corresponding figures at doubled CO<sub>2</sub> are 1.46 K and 4.0%, respectively. Hence, the global climate responses to these sources of forcing are nearly additive. The increase in surface temperature due to the combined effect of anthropogenic aerosols and a doubling of CO<sub>2</sub> is 1.15 K, compared to 1.17 K for the sum of the two effects. This result contrasts that of Feichter et al. (2004), who found a considerably weaker global warming for combined aerosol and CO<sub>2</sub> forcing than obtained by adding the individual responses.

Apart from a southward shift in the ITCZ as a response to the asymmetric interhemispheric distribution of aerosol forcing, the spatial climate response patterns differ considerably from the forcing patterns both for aerosols and CO<sub>2</sub>. Feedbacks related to ice and snow cover, as well as clouds, generally produce high-latitude amplification of the temperature signals. The presented

results emphasize that the climate system's response pattern is only partly determined by the detailed structure of the forcing, and generally more by the properties of local feedbacks and naturally occurring flow regimes in the climate system.

The cooling by anthropogenic aerosols is predominantly due to the indirect forcing of sulphate. While being a magnitude smaller at the TOA, the direct forcing is about half of the first indirect forcing at the ground. This is due to solar absorption by BC particles, which exert a negative forcing at the surface but a positive forcing on the atmospheric column. Changing aerosol emissions from present-day to projected SRES A2 emissions for the year 2100 gives a doubling of the BC burden whilst sulphate is only slightly increased and shifted southwards. This leads to a 0.3 K surface air warming, compared to what is found for present-day aerosols, thus *enhancing* the global warming from greenhouse gases. The warming due to increased BC is largest in the Northern Hemisphere, and the southward shift in ITCZ due to aerosol forcing is partly reversed. The net increase in globally averaged precipitation is small despite the considerable rise in temperature, only 0.1%. This is probably caused by a weakening of the hydrological cycle in response to the negative ground surface forcing of BC mentioned above.

To summarize, our simulations indicate that the global warming and the associated increase in precipitation up to now would be considerably larger without the effects of anthropogenic aerosols, as expected. However, the results suggest that this tendency of anthropogenic aerosols to counteract the effects of enhanced greenhouse gas levels may be reversed in the future, since light-absorbing BC is projected to increase compared to soluble and light-scattering aerosols such as sulphate. This applies to the response in surface air temperatures, and to a lesser extent also the precipitation.

Although the precipitation response to *present-day* anthropogenic aerosols and increased CO<sub>2</sub>-levels counteract each other in a globally averaged sense, there are large spatial variations. The presented results suggest that also these aerosols may enhance the response of the CO<sub>2</sub> forcing regionally, namely in parts of the tropics. Hence, any effort to offset the enhanced greenhouse warming by simply maintaining high aerosol emissions may aggravate the situation in parts of the world, by leading to more intense and more frequent droughts or floods.

Defined as the global precipitation change normalized by the global surface air temperature change, the equilibrium hydrological sensitivity is estimated at about 3.0% K<sup>-1</sup> for present-day anthropogenic aerosols, while for a doubling of CO<sub>2</sub> a value of 1.8% K<sup>-1</sup> is obtained, close to the 1.9% K<sup>-1</sup> given in IPCC (2001). Although it is almost 70% larger for aerosols than for CO<sub>2</sub>, the joint hydrological sensitivity to changes in aerosols and CO<sub>2</sub> is slightly positive: 0.30% K<sup>-1</sup>. For anthropogenic aerosols in the 2100 emission scenario, in which both anthropogenic aerosols and CO<sub>2</sub> contribute to a global warming relative to present-day, the hydrological sensitivity is close to that of CO<sub>2</sub> alone.

Although our radiative forcing estimates for the direct effect and the first indirect effect (radius effect) are within the range given in IPCC (2001 and 2007), the estimated cooling due to the indirect effect, especially over land, is probably exaggerated in CCM-Oslo. This problem is being dealt with by introducing various major improvements to the parametrization schemes, and by using CAM2/CAM3 instead of CCM3 as a host model. For instance, in Storelvmo et al. (2006b) the treatment of the aerosol indirect effects has been greatly improved by introducing a prognostic equation for cloud droplet number concentrations, explicitly accounting for microphysical sources and sinks, and with organic carbon (OC) aerosols included (Kirkevåg et al., 2005). This new treatment of cloud droplet numbers yields a considerably smaller aerosol indirect forcing than obtained with CCM-Oslo. The latest CAM-Oslo version, based on CAM3, currently does not include the prognostic equation for cloud droplet number, but has a more sophisticated aerosol life cycle scheme, equipped with fully prognostic mineral, sea-salt and OC aerosols in addition to sulphate and BC (Seland et al., 2008). Equilibrium response simulations with that version of CAM-Oslo coupled to a slab ocean model are presented in Kirkevåg et al. (2008). Implementation and further development of the prognostic cloud droplet number scheme into that version of CAM-Oslo is ongoing.

## 6. Acknowledgments

This study was supported by the Norwegian Research Council through the RegClim and AeroOzClim projects, and partly through the NorClim project in 2007. Furthermore, the work has received support of the Norwegian Research Council's Programme for Supercomputing through a grant of computer time.

## References

- Andreae, M. O., Jones, C. D. and Cox, P. M. 2005. Strong present-day aerosol cooling implies a hot future. *Nature* **435**, 1187–1190.
- Boer, G. J. and Yu, B. 2003. Climate sensitivity and response. *Clim. Dyn.* **20**, 415–429, doi:10.1007/s00382-002-0283-3.
- Broccoli, A. J., Dahl, K. A. and Stouffer, R. J. 2006. Response of the ITCZ to Northern Hemispheric cooling. *Geophys. Res. Lett.* **33**, L01702, doi:10.1029/2005GL024546.
- Chung, S. H. and Seinfeld, J. H. 2005. Climate response of direct radiative forcing of anthropogenic black carbon. *J. Geophys. Res.* **110**, D11102, doi:10.1029/2004JD005441.
- Corti, S., Molenti, F. and Palmer, T. N. 1999. Signature of recent climate change in frequencies of natural atmospheric circulation regimes. *Nature* **398**, 799–802.
- Feichter, J., Roekner, E., Lohmann, U. and Liepert, B. 2004. Nonlinear aspects of the climate response to greenhouse gas and aerosol forcing. *J. Climate* **17**, 2384–2398.
- Hack, J. J., Kiehl, J. T. and Hurrell, J. W. 1998. The hydrologic and thermodynamic characteristics of the NCAR CCM3. *J. Climate* **11**, 1179–1206.
- Hegerl, G. C., Zwiers, F. W., Braconnot, P., Gillett, N. P., Luo, Y., and co-authors. 2007. Understanding and Attributing Climate Change. In *Climate Change 2007: The Physical Science Basis. Contribution of Working Group I to the Fourth Assessment Report of the Intergovernmental Panel on Climate Change* (eds S. Solomon, D. Qin, M. Manning, Z. Chen, M. Marquis, K. B. Averyt, M. Tignor and H. L. Miller), Cambridge University Press, Cambridge, United Kingdom and New York, NY, USA.
- IPCC. 2001. *Climate Change 2001: The Scientific Basis*. Contribution of Working Group I to the Third Assessment Report of the Intergovernmental Panel on Climate Change (eds J. T. Houghton, Y. Ding, D. J. Griggs, M. Noguer, P. J. van der Linden, X. Dai, K. Maskell and C. A. Johnson), Cambridge University Press, 881 pp.
- IPCC. 2007. *Climate Change 2007: The Physical Science Basis Summary for Policymakers*. Contribution of Working Group I to the Fourth Assessment Report of the Intergovernmental Panel on Climate Change. WMO, Geneva, Switzerland, 18 pp.
- Iversen, T. and Seland, Ø. 2002. A scheme for process-tagged SO<sub>4</sub> and BC aerosols in NCAR-CCM3. Validation and sensitivity to cloud processes. *J. Geophys. Res.* **107**(D24), 4751, doi:10.1029/2001JD000885.
- Iversen, T. and Seland, Ø. 2003. Correction to “A scheme for process-tagged SO<sub>4</sub> and BC aerosols in NCAR-CCM3. Validation and sensitivity to cloud processes”. *J. Geophys. Res.* **108**(D16), 4502, doi:10.1029/2003JD003840.
- Iversen, T., Kristjánsson, J. E., Kirkevåg, A. and Seland, Ø. 2005. Calculated feedback effects of climate change caused by anthropogenic aerosols. *RegClim General Technical Report No. 8*, 111–120.
- Iversen, T., Kristiansen, J., Jung, T. and Barkmeijer, J. 2008. Optimal atmospheric forcing perturbations for the cold ocean warm land pattern *Tellus* **60A**, 10.1111/j.1600-0870.2008.00310.x.
- Kanakidou, M., Seinfeld, J. H., Pandis, S. N., and co-authors. 2005. Organic aerosol and climate modelling: a review. *Atmos. Chem. Phys.* **5**, 1053–1123.
- Kiehl, J. T., Hack, J. J., Bonan, G. B., Boville, B. A., Briegleb, B. P., and co-authors. 1996. *Description of the NCAR Community Climate Model (CCM3)*. NCAR Technical Note, NCAR/TN-420+STR, 152 pp.
- Kiehl, J. T., Hack, J. J., Bonan, G. B., Boville, B. A., Williamson, D. L., and co-authors. 1998. The National Center for Atmospheric Research Community Climate Model: CCM3. *J. Climate* **11**, 1131–1149.
- Kiehl, J. T., Schields, C. A., Hack, J. J. and Collins, W. D. 2006. The climate sensitivity of the Community Climate System Model: CCSM3. *J. Climate* **19**, 2584–2596.
- Kirkevåg, A. and Iversen, T. 2002. Global direct radiative forcing by process-parameterized aerosol optical properties. *J. Geophys. Res.* **107**(D20), 4433, doi:10.1029/2001JD000886.
- Kirkevåg, A., Iversen, T., Seland, Ø. and Kristjánsson, J. E. 2005. Revised schemes for aerosol optical parameters and cloud condensation nuclei in CCM-Oslo. *Institute Report Series*, Department of Geosciences, University of Oslo, 29 pp, ISBN 82-91885-31-1, ISSN 1501-6854-128.
- Kirkevåg, A., Iversen, T., Seland, Ø., Debernard, J. B., Storelvmo, T., and co-authors. 2008. Aerosols and aerosol-cloud-climate interactions in the climate model CAM-Oslo. *Tellus* **60A**, this issue.
- Kristjánsson, J. E. 2002. Studies of the aerosol indirect effect from sulfate and black carbon aerosols. *J. Geophys. Res.* **107**(D15), 4246, doi:10.1029/2001JD000887.

- Kristjánsson, J. E., Iversen, T., Kirkevåg, A., Seland, Ø. and Debernard, J. 2005. Response of the climate system to aerosol direct and indirect forcing: role of cloud feedbacks. *J. Geophys. Res.* **110**, D24206, doi:10.1029/2005JD006299.
- Legates, D. R. and Willmott, C. J. 1990. Mean seasonal and spatial variability in global surface air temperature. *Theor. Appl. Climatol.* **41**, 11–21.
- Lohmann, U. and Feichter, J. 2005. Global indirect aerosol effects: a review. *Atmos. Chem. Phys.* **5**, 715–737.
- Meehl, G. A., Collins, W. D., Boville, B. A., Kiehl, J. T., Wigley, T. M. L., and co-authors. 2000. Response of the NCAR Climate System Model to increased CO<sub>2</sub> and the role of physical processes. *J. Climate* **13**, 1879–1898.
- Menon, S., A. DelGenio, D., Koch, D. and Tselioudis, G. 2002. GCM simulations of the aerosol indirect effect: sensitivity to cloud parameterization and aerosol burden. *J. Atmos. Sci.* **59**, 692–713.
- Palmer, T. N. 1999. A nonlinear dynamical perspective on climate prediction. *J. Climate* **12**, 575–591.
- Penner, J. E. (co-ordinating lead author). 2001. *Aerosols, Their Direct and Indirect Effects*. Chapter 5 in the Third Assessment Report of the Intergovernmental Panel on Climate Change. Cambridge University Press, 291–348.
- Penner, J. E., Quaas, J., Storelvmo, T., Takemura, T., Boucher, O., and co-authors. 2006. Model intercomparison of indirect aerosol effects. *Atm. Chem. Phys.* **6**, 3391–340
- Quaas, J., Boucher, O. and Lohmann, U. 2006. Constraining the total aerosol indirect effect in the LMDZ and ECHAM4 GCMs using MODIS satellite data. *Atmos. Chem. Phys.* **6**, 947–955.
- Ramaswamy, V. (co-ordinating lead author). 2001. *Radiative Forcing of Climate Change*. Chapter 6 in the Third Assessment Report of the Intergovernmental Panel on Climate Change. Cambridge University Press, pp. 349–416.
- Rasch, P. J. and Kristjánsson, J. E. 1998. A comparison of the CCM3 model climate using diagnosed and predicted condensate parameterizations. *J. Climate* **11**, 1587–1614.
- Rossow, W. B. and Schiffer, R. A. 1999. Advances in understanding clouds from ISCCP. *Bull. Am. Meteorol. Soc.* **80**, 2261–2287.
- Randall, D. A., Wood, R. A., Bony, S., Colman, R., Fife, T., and co-authors. 2007. Climate models and their evaluation. In: *Climate Change 2007: The Physical Science Basis. Contribution of Working Group I to the Fourth Assessment Report of the Intergovernmental Panel on Climate Change* (eds S. Solomon, D. Qin, M. Manning, Z. Chen, M. Marquis, K. B. Averyt, M. Tignor and H. L. Miller), Cambridge University Press, Cambridge, United Kingdom and New York, NY, USA.
- Rotstayn, L. D. and Lohmann, U. 2002. Tropical rainfall trends and the indirect aerosol effect. *J. Climate* **15**, 2103–2116.
- Rotstayn, L. D., Ryan, B. F. and Penner, J. E. 2000. Precipitation changes in a GCM resulting from the indirect effects of anthropogenic aerosols. *Geophys. Res. Lett.* **27**, 3045–3048.
- Rotstayn, L. D., Cai, W., Dix, M. R., Farquhar, G. D., Feng, Y., and co-authors. 2007. Have Australian rainfall and cloudiness increased due to the remote effects of Asian anthropogenic aerosols. *J. Geophys. Res.* **112**, D09202, doi:10.1029/2006JD007712.
- Schulz, M., Textor, C., Kinne, S., Balkanski, Y., Bauer, S., and co-authors. 2006. Radiative forcing by aerosols as derived from the AeroCom present-day and pre-industrial simulations. *Atmos. Chem. Phys.* **6**, 5225–5246.
- Seinfeld, J. H. and Pandis, S. N. 1998. *Atmospheric Chemistry and Physics: From Air Pollution to Climate Change*, John Wiley, New York, 1326 pp.
- Seland, Ø., Iversen, T., Kirkevåg, A. and Storelvmo, T. 2008. Aerosol-climate interactions in the CAM-Oslo atmospheric GCM and investigation of associated basic shortcomings. *Tellus* **60A**, this issue.
- Shine, K. P., Cook, J., Highwood, E. H. and Joshi, M. M. 2003. An alternative to radiative forcing for estimating the relative importance of climate change mechanisms. *Geophys. Res. Lett.* **30**(20), 2047, doi:10.1029/2003GL018141.
- Stocker, T. F., Clarke, G. K. C., Le Treut, H., Lindzen, R. S., Meleshko, V. P., and co-authors. 2001. Physical climate processes and feedbacks. In: *Climate Change 2001: The Scientific Basis*. Cambridge University Press, Cambridge, UK, 417–470.
- Storelvmo, T., Kristjánsson, J. E., Myhre, G., Johnsrud, M. and Stordal, F. 2006a. Combined observational and modeling based study of the aerosol indirect effect (COMBINE). *Atmos. Chem. Phys.* **6**, 3583–3601.
- Storelvmo, T., Kristjánsson, J. E., Ghan, S., Kirkevåg, A., Seland, Ø., and co-authors. 2006b. Predicting cloud droplet number in CAM-Oslo. *J. Geophys. Res.* **111**, D24208, doi:10.1029/2005JD006300.
- Takemura, T., Nozawa, T., Emori, S., Nakajima, T. Y. and Nakajima, T. 2005. Simulation of climate response to aerosol direct and indirect effects with aerosol transport-radiation model. *J. Geophys. Res.* **110**, D02202, doi:10.1029/2004JD005029.
- Teng, H., Buja, L. E. and Meehl, G. A. 2006. Twenty-first century climate change commitment from a multi-model ensemble. *Geophys. Res. Lett.* **33**, L07706, doi:10.1029/2005GL024766.
- Textor, C., Schulz, M., Guibert, S., Kinne, S., Balkanski, Y., and co-authors. 2006. Analysis and quantification of the diversities of aerosol life cycles within AeroCom. *Atmos. Chem. Phys.* **6**, 1777–1813.
- von Storch, H. and Zwiers, F. W. 1999. *Statistical Analysis in Climate Research*. Cambridge University Press, Cambridge, UK, 484 pp.
- Wallace, J. M., Zhang, Y. and Bajuk, L. 1996. Interpretation of interdecadal trends in Northern Hemispheric surface air temperature. *J. Climate* **9**, 249–259.
- Warren, S. G., Hahn, C. J., London, J., Chervin, R. M. and Jenne, R. L. 1988. *Global Distribution of Cloud Cover and Cloud Type Amounts Over the Ocean*, NCAR Technical Note, National Center for Atmospheric Research, Boulder, Colorado.
- Williams, K. D., Jones, A., Roberts, D. L., Senior, C. A. and Woodage, M. J. 2001. The response of the climate system to the indirect effects of anthropogenic sulfate aerosol. *Clim. Dyn.* **17**, 845–856.
- Zhang, C. 2001. Double ITCZs. *J. Geophys. Res.* **106**(D11), 11785–11792.
- Zhang, G. J. and Wang, H. 2006. Toward mitigating the double ITCZ problem in NCAR CCSM3. *Geophys. Res. Lett.* **33**, L06709, doi:10.1029/2005GL025229.